Draft version February 5, 2008
Preprint typeset using LaTeX style emulateapj v. 6/22/04

arXiv:astro-ph/0601477v2 23 Jan 2006

SPECTROSCOPIC IDENTIFICATION OF COOL WHITE DWARFS IN THE SOLAR NEIGHBOURHOOD

Adela Kawka
Astronomický ústav AV ČR, Fričova 298, 251 65 Ondřejov, Czech Republic

and

Stéphane Vennes
Department of Physics and Space Sciences, Florida Institute of Technology, 150 W University Blvd., Melbourne, FL 32901-6975

Draft version February 5, 2008

ABSTRACT

The New Luyten Two-Tenths catalog contains a large number of high-proper motion white dwarf candidates that remain to be spectroscopically confirmed. We present new spectroscopic observations as well as SDSS archival spectra of 49 white dwarf candidates which have been selected from the revised NLTT catalog of Salim & Gould (2003). Out of these, 34 are cool DA white dwarfs with temperatures ranging from approximately 5000 K up to 11690 K, and 11 are DC white dwarfs with temperatures ranging from 4300 K (NLTT 18555) up to 11000 K. Three of the DA white dwarfs also display abundances of heavy elements (NLTT 3915, NLTT 44986 and NLTT 43806) and one is a cool magnetic white dwarf (NLTT 44447) with an estimated magnetic field strength of 1.3 MG. We also present a new cool DQ white dwarf (NLTT 31347) with an estimated temperature of 6250 K. We supplement our sample with SDSS *ugriz* photometry for a fraction of the newly identified white dwarfs. A kinematical study of this sample of white dwarfs, characterized by proper motions ranging from 0.136 to 0.611″yr^{-1} suggest that they belong to the thin disk population.

Subject headings: solar neighborhood – stars: atmospheres– white dwarfs

1. INTRODUCTION

The current census of white dwarfs in the solar neighborhood is believed to be complete only to about 13 pc, and is measurably incomplete within 20 pc (Holberg et al. 2002; Schröder et al. 2004). The local sample of white dwarfs appears to be an old population consisting of mostly cool white dwarfs. The average absolute magnitude for the local census of white dwarfs is $M_V = 13.7$ which corresponds to a temperature of ~ 7000 K. A significant fraction of white dwarfs within 13 pc (Kawka et al. 2003, $20 \pm 8\%$) show the presence of a magnetic field. Holberg et al. (2002) determined that over a quarter of the white dwarfs within 20 pc are in binary systems. Based on recent literature, we updated the spectral classifications of the sample of white dwarfs within 20 pc (Holberg et al. 2002) and found that about 70% of the stars are hydrogen-rich. The remaining 30% are helium-rich, and out of these helium rich white dwarfs about half are DC white dwarfs, about a third are cool DQ white dwarfs, while the remainder are DZ white dwarfs.

The New Luyten Two-Tenths (NLTT) catalog has been used to search for nearby cool dwarfs and subdwarfs (Gizis & Reid 1997; Reid et al. 2003; Yong & Lambert 2003; Reid & Gizis 2005) and for white dwarfs (Liebert & Strittmatter 1977; Hintzen 1986; Vennes & Kawka 2003; Kawka et al. 2004; Kawka & Vennes 2005). However, a large number of objects still require a formal spectroscopic confirmation. Recently, Salim & Gould (2003) have revised the coordinates and proper motions of most stars in the NLTT catalog by cross-correlating the catalog with the Two Micron All Sky Survey (2MASS) and the USNO-A catalogs. One problem with the original catalog was that there was no obvious separation between different populations because the R and B photographic bands do not provide a broad enough baseline to distinguish between main-sequence, subdwarf and white dwarf populations. Salim & Gould (2002) showed that using an optical/infrared $(V - J)$ reduced proper motion diagram they could distinguish between these groups of stars and from this diagram they listed 23 white dwarf candidates within 20 pc from the Sun. Vennes & Kawka (2003) and Kawka et al. (2004) found that only a third of these nearby candidates are white dwarfs, with the remainder being cool red dwarfs and subdwarfs.

Recently, several projects have been initiated to search for high-proper motion stars, such as the SuperCOSMOS-RECONS survey (Hambly et al. 2004) and LSPM Catalog (Lepine & Shara 2005) which utilizes the SuperCOSMOS Sky Survey (Hambly et al. 2001) and SUPERBLINK (Lepine et al. 2002), respectively. These surveys have detected many high-proper motion stars which are either nearby or have been labeled as halo candidates. One such object is the cool white dwarf WD 0346+246 (Hambly et al. 1997), which has definite halo kinematics and is very cool ($T \sim 3800$ K) and hence old enough to belong to the halo. A total of 299 new stars with $0.4''$ yr^{-1} have been discovered using the SuperCosmos-RECONS survey (Subasavage et al. 2005), out of which 148 have proper motions greater than $0.5''$yr^{-1} and 43 are within 25 pc from the Sun. Lepine et al. (2002, 2003) reported the discovery of 198 new stars with proper motions greater than $0.5''$yr^{-1} using SUPERBLINK. Their survey also included the nearby halo white dwarf PM J13420−3415 (Lepine et al. 2005).

The NLTT catalog appears to be complete at Galactic latitudes $|b| > 15°$, however at low Galactic latitudes the catalog appears to be significantly incomplete. On the other hand, Salim & Gould (2003) notes that

the completeness for white dwarfs is very high, i.e., the coverage of white dwarfs appears to be completely uniform. The reason for this may be that Luyten concentrated on blue objects, which are no more common in the plane than elsewhere, and hence Luyten was able to detect most high-proper motion white dwarfs above $\delta > -32.5°$. Another survey to search for cool white dwarfs with high-proper motion using the Guide Star Catalog II was initiated by Carollo et al. (2005) with the aim of placing constraints on the halo white dwarf space density. Their search resulted in the discovery of 24 new white dwarfs. Many earlier proper motion surveys, in particular the Luyten proper motion surveys relied on plate pairs taken a decade or more apart, and very high-proper motion stars were most likely lost in the background. A search for ultra-high proper motion stars was performed by Teegarden et al. (2003) using the SkyMorph database of the Near Earth Asteroid Tracking (NEAT) project (Pravdo et al. 1999) and found a main-sequence star with spectral type M6.5 and with a proper motion of $5.05'' \pm 0.03''\mathrm{yr}^{-1}$ at a distance of $2.4^{+0.7}_{-0.4}$ pc which they obtained from the trigonometric parallax.

Since most of the stars in the NLTT catalog are brighter than 19th magnitude, we do not expect to find many halo white dwarf candidates. Since the halo star formation history is assumed to be a burst occurring 12 Gyrs ago, then most of the halo white dwarfs would be required to have cooling ages greater than 10 Gyrs (and hence $M_V \gtrsim 16$). Given that the percentage of halo white dwarfs in the local population is $\sim 2\%$ (Pauli et al. 2005), then most halo candidates are likely to be at large distances and hence too faint to be included in the NLTT catalog.

In this paper, we pursue our study of white dwarf candidates (Kawka et al. 2004) from the revised NLTT (rNLTT) catalog of Salim & Gould (2003). Some preliminary results were presented in Kawka & Vennes (2005). We present the list of white dwarfs observed in §2 and their spectroscopic observations in §2.1 with complementary optical and infrared photometric data presented in §2.2. The model atmospheres and spectra we used to analyze our data are described in §3 and in §4 we present our analysis of the new white dwarf stars. We discuss our findings in §5 and summarize in §6.

2. OBSERVATIONS OF WHITE DWARF CANDIDATES

Table 1 lists the white dwarf candidates for which we have obtained a spectroscopic identification. Many of the white dwarfs were listed in the Luyten White Dwarf Catalogs (LWDC) (Luyten 1970, 1977), and required spectroscopic confirmation of their classification.

2.1. *Spectroscopy*

The rNLTT white dwarf candidates were observed using the Dual Imaging Spectrogram (DIS) attached to the 3.5 m telescope at the Apache Point Observatory (APO) on 2004 May 31, June 1, 2005 May 12, 16, June 2, July 2, 15, August 9 and November 12, 14. We used 300 lines/mm gratings to obtain a spectral range of 3700 to 5600 Å with a dispersion of 2.4 Å per pixel in the blue, and a spectral range of 5300 to 9800 Å with a dispersion of 2.3 Å in the red.

We also obtained spectroscopy by cross-correlating the list of rNLTT white dwarf candidates with the Sloan Digital Sky Survey (SDSS). We used the archival spectra from the 4th Data Release of SDSS in our analyses of these objects.

Figure 1 shows the spectra of all the hydrogen-rich white dwarfs, and Figure 2 shows the spectra of the helium-rich white dwarfs obtained at APO.

2.2. *Photometry*

Table 1 lists the V magnitudes and JHK photometry for the rNLTT white dwarf candidates for which we have obtained spectroscopy. The table also lists the stars' alternate names and their proper motion taken from rNLTT catalog of Salim & Gould (2003). The V magnitudes are taken from the rNLTT catalog of Salim & Gould (2003), except for stars where more accurate photometry from another source was available. The JHK photometry was obtained from the 2MASS database available at the Centre de Données Astronomique de Strasbourg. The data were converted from 2MASS system to the CIT system using color transformations provided by Cutri et al. (2003). [1]

We cross-correlated the list of rNLTT white dwarf candidates with the SDSS to obtain *ugriz* photometry (Table 2).

3. MODEL ATMOSPHERES AND SPECTRA

The stars presented in this paper have been analyzed for their $T_{\rm eff}$, $\log g$ using a grid of computed pure hydrogen LTE plane-parallel models. The grid of models extend from $T_{\rm eff} = 4500$ to 6500 K (in steps of 500 K) at $\log g = 7.0, 8.0$ and 9.0, from $T_{\rm eff} = 7000$ to 16000 K (in steps of 1000 K), from 18000 to 32000 K (in steps of 2000 K) and from 36000 to 84000 K (in steps of 4000 K) at $\log g = 7.0$ to 9.5 (in steps of 0.25 dex). Convective energy transport in cooler atmospheres is included by applying the Schwartzschild stability criterion and by using the mixing length formalism described by Mihalas (1978). We have assumed the ML2 parameterization of the convective flux (Fontaine et al. 1981) and adopting $\alpha = 0.6$ (Bergeron et al. 1992), where α is the ratio of the mixing length to the pressure scale height. The equation of convective energy transfer was fully linearized within the Feautrier solution scheme and subjected to the constraint that $\mathcal{F}_{\rm total} = \sigma_R T_{\rm eff}^4 = \mathcal{F}_{\rm conv} + \mathcal{F}_{\rm rad}$, where $\mathcal{F}_{\rm conv}$ is the convective flux and $\mathcal{F}_{\rm rad}$ is the radiative flux.

The dissolution of the hydrogen energy levels in the high-density atmospheres of white dwarfs was calculated using the formalism of Hummer & Mihalas (1988, hereafter HM) and following the treatment of Hubeny et al. (1994, hereafter HHL)). For the sake of reproducibility we now provide details of the calculations as included in our fortran code. That is we calculated the occupation probability from charged particles of level n using the form (HM Eq. 4.26 and HHL Eq. A.2):

$$w_n(\text{charged}) = Q(\beta_n) = \int_0^\beta W(\beta) d\beta. \qquad (1)$$

$W(\beta)$ is the Holtzmark distribution function. β can be calculated using:

$$\beta = K_n \Big(\frac{Z^3}{16n^4}\Big)\Big(\frac{4\pi a_0}{3}\Big)^{-\frac{2}{3}} N_e^{-1} N_{\rm ion}^{\frac{1}{3}}, \qquad (2)$$

[1] Available on the World Wide Web at http://www.ipac.caltech.edu/2mass/releases/allsky/doc/explsup.html.

TABLE 1
NLTT White Dwarfs

NLTT	Alternate Names	μ,θ[a] ($''$ yr^{-1},deg)	V (mag)	$V-J$[b] (mag)	$J-H$[b] (mag)
287	LP 464-57	0.424, 124.0	16.02 ± 0.2[a]	0.91 ± 0.50	0.026 ± 0.100
529	GD 5, LP 192-41	0.237, 193.4	15.23 ± 0.2[a]	0.68 ± 0.37	0.214 ± 0.067
3022	G 240-93, PHL 3101	0.210, 268.9	16.67 ± 0.2[a]	0.02 ± 3.22	-0.362 ± 1.027
3915	LP 294-61	0.227, 219.3	16.15 ± 0.2[a]	0.91 ± 0.54	0.211 ± 0.128
6275	G 72-40, G94-21	0.213, 76.6	15.77 ± 0.2[a]	0.67 ± 0.56	0.035 ± 0.121
8435	LHS 1421	0.611, 190.0	15.74 ± 0.07[c]	1.28 ± 0.27	0.144 ± 0.081
8581	G 36-29	0.340, 117.0	16.29 ± 0.2[a]	1.37 ± 0.40	0.327 ± 0.077
8651	GD 32	0.172, 235.7	16.23 ± 0.2[a]	0.73 ± 0.50	0.292 ± 0.118
9933	LP 299-22	0.190, 119.6	15.83 ± 0.2[a]	-0.76 ± 1.07	0.035 ± 0.335
10398	GD 44	0.176, 153.7	15.74 ± 0.2[a]	0.19 ± 0.71	0.034 ± 0.166
14307	G 84-26	0.293, 142.9	15.30 ± 0.2[a]	-0.05 ± 0.58	0.160 ± 0.123
14352	LP 656-32	0.239, 157.6	16.80 ± 0.2[a]	0.76 ± 0.71	0.063 ± 0.200
17285	LP 661-15	0.211, 312.2	16.73 ± 0.2[a]	0.84 ± 0.74	0.513 ± 0.186
18555	LP 207-50	0.420, 165.8	17.45 ± 0.2[a]	1.70 ± 1.63	-0.029 ± 0.251
18642	LP 207-55, KUV 07531+4148	0.322, 181.4	16.56 ± 0.2[a]	0.56 ± 0.83	0.177 ± 0.228
19019	LP 311-2, GD 262	0.182, 113.3	16.09 ± 0.2[a]	0.65 ± 0.55	0.065 ± 0.126
19138	G 111-64	0.258, 166.5	15.74 ± 0.2[a]	1.41 ± 0.37	0.213 ± 0.068
20165	KUV 08422+3813	0.217, 152.4	16.03 ± 0.2[a]	0.52 ± 0.62	0.081 ± 0.138
21241	LP 210-58	0.200, 258.6	17.27 ± 0.2[a]	0.87 ± 1.66	0.310 ± 0.276
27901	GD 311, LP 94-285, LB 2052	0.232, 238.7	16.66 ± 0.2[a]	0.62 ± 0.80	0.156 ± 0.212
28772	LP 129-587, G197-35	0.300, 266.8	16.67 ± 0.2[a]	0.15 ± 1.73	0.210 ± 0.306
28920	LP 19-411	0.282, 209.3	15.90 ± 0.2[a]	0.20 ± 0.91	0.062 ± 0.237
29233	G122-61, CBS 451	0.300, 262.8	16.00 ± 0.2[a]	0.77 ± 0.52	0.044 ± 0.103
30738	LP 435-109	0.162, 260.8	16.19 ± 0.2[a]	0.37 ± 0.75	0.384 ± 0.189
31347	LP217-47, LHS 5222	0.506, 315.0	17.53 ± 0.2[a]	0.96 ± 1.65	0.084 ± 0.259
31748	PG 1242-106	0.349, 257.1	14.43 ± 0.2[a]	0.19 ± 0.35	0.194 ± 0.057
32390	LP 96-9	0.233, 243.3	17.57 ± 0.2[a]	1.42 ± 0.62	0.673 ± 0.188
32695	LP 616-70	0.190, 271.9	16.84 ± 0.2[a]	0.40 ± 3.22	0.408 ± 1.026
34264	LP 617-70	0.230, 175.5	16.46 ± 0.2[a]	0.03 ± 1.59	0.247 ± 0.233
34564	LP 678-8	0.245, 280.3	16.40 ± 0.2[a]	0.77 ± 0.68	0.155 ± 0.159
35880	LP 97-430	0.309, 281.0	17.63 ± 0.2[a]	0.91 ± 1.63	1.121 ± 0.282
38499	LP 801-14, EC 14473-1901	0.269, 288.0	15.80 ± 0.02[d]	0.73 ± 0.29	0.215 ± 0.094
40489	LP 503-7, GD 184	0.179, 177.2	16.56 ± 0.2[a]	0.43 ± 1.58	0.226 ± 0.228
40607	G 137-24	0.248, 221.6	15.07 ± 0.05[e]	0.12 ± 0.25	0.237 ± 0.076
40881	LP 273-64, LTT 14655, GD 187	0.186, 295.4	15.03 ± 0.2[a]	0.24 ± 0.40	0.107 ± 0.084
40992	LP 384-38	0.417, 173.2	16.95 ± 0.2[a]	1.19 ± 0.77	0.302 ± 0.178
41800	G 202-26	0.318, 330.3	16.49 ± 0.2[a]	0.81 ± 0.69	0.113 ± 0.168
42050	LP 274-53	0.255, 172.7	16.95 ± 0.2[a]	1.06 ± 0.71	0.170 ± 0.182
42153	LP 861-31	0.194, 312.4	15.46 ± 0.2[a]	0.35 ± 0.56	0.045 ± 0.126
43806	LP 276-33	0.329, 177.6	15.86 ± 0.2[a]	0.31 ± 0.61	0.211 ± 0.154
43827	LP 387-21	0.208, 164.7	16.90 ± 0.2[a]	0.77 ± 0.79	0.552 ± 0.220
43985	LP 331-27	0.343, 224.8	16.92 ± 0.2[a]	0.42 ± 2.45	-0.091 ± 1.040
44000	G 203-39	0.385, 228.9	16.72 ± 0.2[a]	1.28 ± 0.60	0.266 ± 0.144
44149	LP 276-48	0.250, 135.3	17.98 ± 0.2[a]	1.41 ± 3.24	0.231 ± 1.039
44447	LP 226-48	0.195, 355.4	16.13 ± 0.2[a]	0.49 ± 0.61	0.276 ± 0.141
44986	EG 545, GD 362, PG 1729+371	0.224, 173.1	16.23 ± 0.2[a]	0.05 ± 3.20	0.128 ± 1.005
45344	LP 227-31	0.217, 189.1	17.25 ± 0.2[a]	1.43 ± 1.53	0.158 ± 0.191
45723	LP 228-12	0.334, 2.9	17.26 ± 0.2[a]	1.32 ± 0.76	0.081 ± 0.202
49985	LP 872-20	0.278, 130.0	15.42 ± 0.2[a]	0.51 ± 0.40	0.224 ± 0.076
50029	LP 872-48, BPS CS 22880-0126	0.136, 3.1	15.01 ± 0.06[c]	0.41 ± 0.28	0.012 ± 0.087
51103	LP 637-32	0.291, 209.2	16.59 ± 0.2[a]	0.91 ± 0.80	0.042 ± 0.233
52404	LP 930-61	0.234, 44.0	16.26 ± 0.17[c]	1.05 ± 0.46	0.115 ± 0.104
53177	LP 759-50, HE 2209-1444	0.267, 70.4	15.09 ± 0.02[f]	0.59 ± 0.23	0.134 ± 0.084
53447	LP 287-39	0.463, 79.3	16.99 ± 0.2[a]	1.57 ± 0.57	0.236 ± 0.136
53468	LP 619-64, PHL 218	0.249, 72.0	15.3 ± 0.2[a]	-0.57 ± 0.90	-0.025 ± 0.243
53996	LP 400-6	0.320, 134.9	17.95 ± 0.2[a]	1.59 ± 1.58	0.347 ± 0.235
54047	LHS 3821, LP 520-28	0.538, 68.4	17.82 ± 0.2[a]	1.47 ± 1.57	0.348 ± 0.228
55932	G 275-8, LP 877-69, LTT 9373	0.339, 106.0	13.68 ± 0.06[c]	-0.49 ± 0.26	0.003 ± 0.075
56122	LP 522-17	0.294, 206.3	17.29 ± 0.2[a]	1.39 ± 0.62	0.451 ± 0.155
56805	LP 522-46	0.352, 71.0	15.81 ± 0.2[a]	1.28 ± 0.42	0.173 ± 0.077
58283	LP 463-68	0.225, 148.3	16.57 ± 0.2[a]	0.63 ± 0.71	0.108 ± 0.191

[a] From Salim & Gould (2003).
[b] JHK from 2MASS magnitudes converted to CIT.
[c] From SPM Catalog 2.0.
[d] From Kilkenny et al. (1997).
[e] From Eggen (1968).
[f] From Beers et al. (1992).

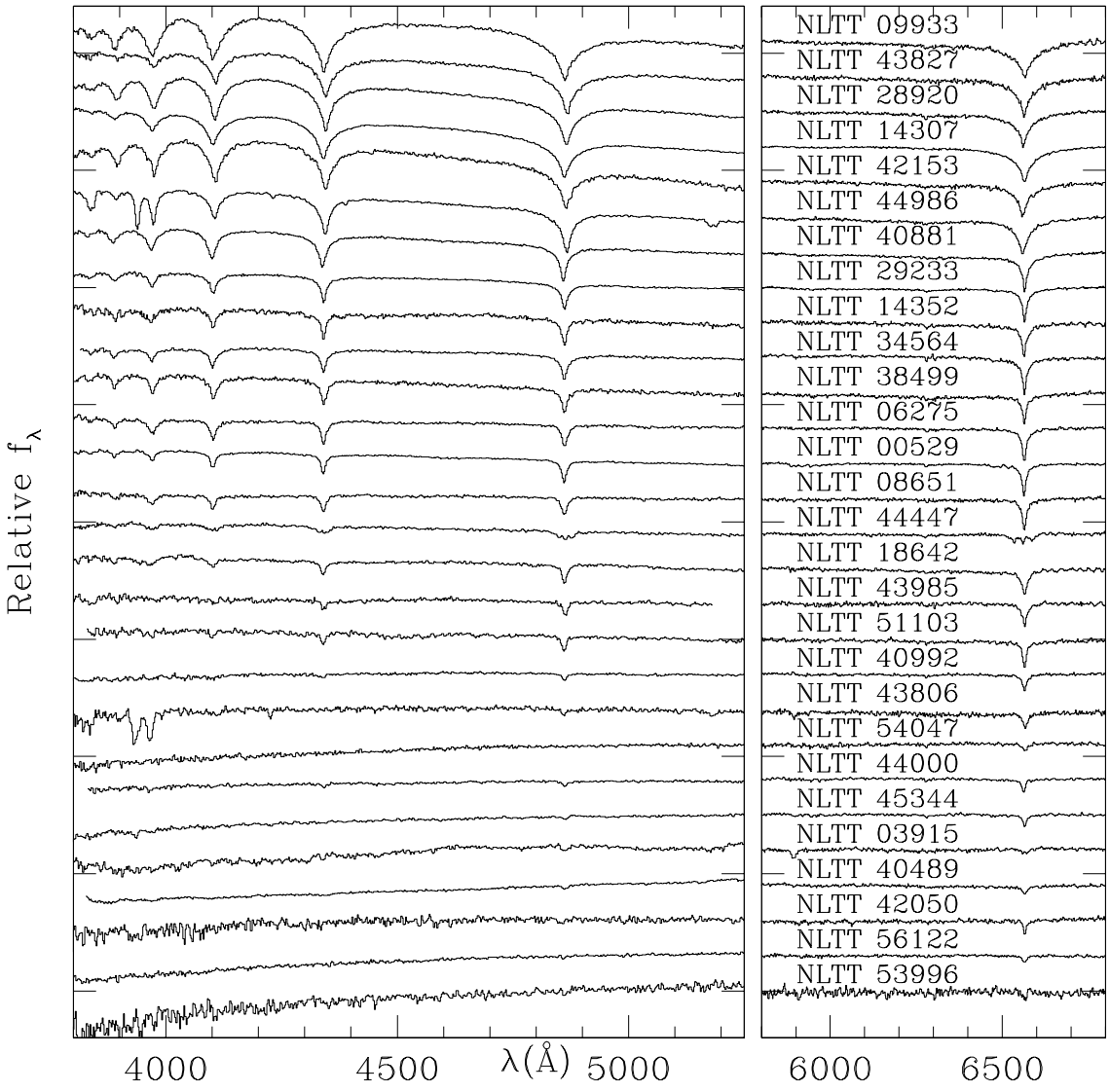

FIG. 1.— APO spectra of NLTT hydrogen-rich white dwarfs.

TABLE 2
SDSS colors of NLTT White Dwarfs

NLTT	SDSS	$u-g$ (mag)	$g-r$ (mag)	$r-i$ (mag)
3022	J005438.84-095219.8	0.404 ± 0.013	0.055 ± 0.008	-0.071 ± 0.009
18555	J075313.27+423001.5	1.929 ± 0.049	0.885 ± 0.011	0.319 ± 0.010
18642	J075631.11+413950.9	0.597 ± 0.013	0.193 ± 0.008	0.073 ± 0.009
19019	J080946.19+292032.1	0.533 ± 0.010	0.170 ± 0.007	0.046 ± 0.008
19138	J081411.16+484529.6	0.562 ± 0.008	0.245 ± 0.006	0.020 ± 0.007
20165	J084524.62+380156.0	0.467 ± 0.010	0.045 ± 0.009	-0.020 ± 0.010
21241	J091356.83+404734.6	0.561 ± 0.016	0.208 ± 0.010	0.047 ± 0.011
27901	J113534.61+572451.7	0.326 ± 0.011	0.086 ± 0.007	-0.031 ± 0.008
28772	J115123.93+541147.7	0.445 ± 0.013	-0.075 ± 0.009	-0.105 ± 0.010
29233	J120003.28+433541.5	0.469 ± 0.010	0.071 ± 0.008	-0.013 ± 0.008
31347	J123752.12+415625.8	0.105 ± 0.018	0.640 ± 0.010	0.257 ± 0.010
32390	J125629.36+610200.9	0.455 ± 0.016	-0.036 ± 0.011	-0.102 ± 0.013
32695	J130247.97-005002.7	0.454 ± 0.013	-0.136 ± 0.011	-0.142 ± 0.013
34264	J132937.15-013430.5	0.526 ± 0.017	0.148 ± 0.010	0.040 ± 0.010
35880	J135758.43+602855.2	0.776 ± 0.028	0.351 ± 0.012	0.106 ± 0.013
40881	J154033.31+330852.8	0.402 ± 0.008	0.000 ± 0.006	-0.077 ± 0.007
40992	J154234.65+232939.8	0.951 ± 0.017	0.391 ± 0.010	0.149 ± 0.010
41800	J160112.70+531700.0	0.613 ± 0.013	0.201 ± 0.008	0.055 ± 0.009
42050	J160714.18+342345.7	1.116 ± 0.025	0.517 ± 0.010	0.183 ± 0.010
43806	J165445.69+382936.5	0.993 ± 0.017	0.417 ± 0.010	0.170 ± 0.010
43827	J165538.92+253345.9	0.225 ± 0.014	-0.106 ± 0.010	-0.159 ± 0.011
43985	J165939.99+320320.0	0.689 ± 0.022	0.291 ± 0.012	0.087 ± 0.012
44149	J170447.70+360847.4	1.832 ± 0.062	0.785 ± 0.014	0.308 ± 0.013
56122	J231206.08+131057.6	1.499 ± 0.030	0.635 ± 0.011	0.225 ± 0.010
56805	J232519.88+140339.7	1.592 ± 0.018	0.598 ± 0.009	0.287 ± 0.010

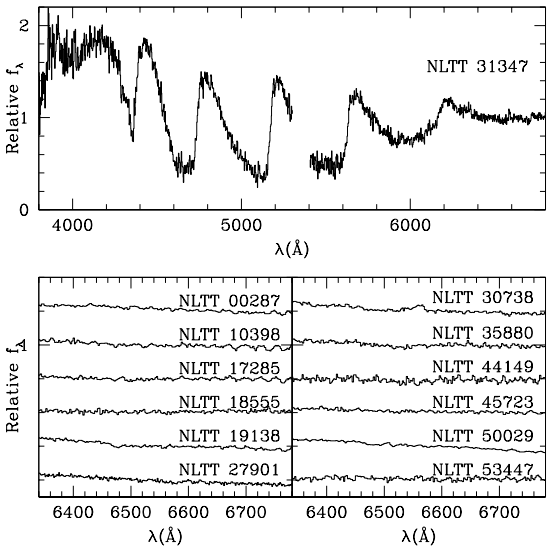

FIG. 2.— Spectra of NLTT helium-rich white dwarfs. *Top:* Spectrum of the DQ white dwarf NLTT31347. *Bottom:* Spectra of the nine new DC white dwarfs. Note the possible weak Hα emission in NLTT 30738.

where Z is the ionic charge, N_e is the electron number density $N_{\rm ion}$ is the ion number density and a_0 is Bohr radius ($a_0 = 0.529 \times 10^{-8}$ cm). And assuming that $N_e = N_{\rm ion}$ we can simplify β to:

$$\beta = 8.59 \times 10^{14} \Big(\frac{K_n Z^3 N_e^{-\frac{2}{3}}}{n^4} \Big). \quad (3)$$

K_n is defined by:

$$K_n = \begin{cases} 1 & \text{for } n \leq 3 \\ \frac{16}{3}\Big(\frac{n}{n+1}\Big)^2 \Big(\frac{n+7/6}{n^2+n+1/2}\Big) & \text{for } n > 3 \end{cases} \quad (4)$$

We can approximate $Q(\beta_n)$ by the rational expression presented by HHL:

$$w_n(\text{charged}) = \frac{f}{1+f}, \quad (5)$$

where f is given by:

$$f = \frac{0.1402(x + 4Za^3)\beta^3}{1 + 0.1285 x \beta^{\frac{3}{2}}}, \quad (6)$$

and $x = (1+a)^{3.15}$ and a is the correlation parameter which is defined as

$$a = f' 0.09 \sqrt{\frac{2}{T}} \Big(\frac{N_e^{\frac{1}{6}}}{1 + \frac{N_{HI}}{N_e}} \Big). \quad (7)$$

Here, T is the temperature and N_{HI} is the number density of neutral hydrogen. We introduced the scaling factor f' to the correlation parameter a which can have values between 0 and 1. In calculating our model spectra we set $f' = 1$. Lowering the value for f' will generate lower values in surface gravity measurements.

HM also considered the contribution to the occupation probability from neutral particles, which is necessary in the case of cool white dwarfs where neutral hydrogen becomes dominant. Therefore, the neutral particle contribution to the occupation probability is given by:

$$w_n = exp\Big(-\frac{4\pi}{3} \sum_m N_m (r_n + r_m)^3 \Big) \quad (8)$$

where we can assume that the effective interaction radius is a fraction f of the hydrogen atomic radius which is associated with level n i.e., $r_n = fn^2a_0$. For our calculations we have assumed $f = 0.5$ (see Bergeron et al. 1991), and therefore

$$w_n = exp\Big(\frac{-\pi a_0^3}{6}\sum_m N_m(n^2+m^2)^3\Big). \quad (9)$$

And finally, the combined occupation probability is the product of the occupation probabilities from neutral and charged particles, i.e.,

$$w_{n,\mathrm{comb}} = w_n(\mathrm{charged}) \times w_n(\mathrm{neutral}) \quad (10)$$

Since the occupation probability depends on the number density of neutral hydrogen N_{HI}, we first obtain an estimate of the populations for all levels by including the contribution from only neutral particles, i.e., $m = 1$. We then repeat the calculations by including the contribution from both neutral and charged particles, until the w_n remains constant for all n.

The calculated level occupation probabilities are then explicitly included in the calculation of the line and continuum opacities. The Balmer line profiles are calculated using the tables of Stark-broadened H I line profiles of Lemke (1997) convolved with normalized resonance line profiles. We have adopted the Stark-broadened line profiles of Lemke (1997) over those of Schöning (1994) because the tables of Lemke (1997) are complete at higher electron densities ($10^{10} \leq n_e \leq 10^{18}$ cm^{-3}). The tables of Schöning (1994) are incomplete at higher electron densities for many lines.

We modeled the heavy element lines using Voigt profiles (Gray 1992) including Stark and van der Waals broadening parameters. In cool DA white dwarfs which display metal lines van der Waals broadening is dominant and the pertubers are neutral hydrogen atoms. For atmospheres dominated by hydrogen, we have used an approximation of the damping constant, γ as defined by Gray (1992):

$$\log\gamma_6 = 19.6 + 0.4\log C_6(H) + \log P_g - 0.7\log T \quad (11)$$

where P_g is the pressure, T is the temperature and $C_6(H)$ can be calculated using:

$$C_6(H) = 0.3\times10^{-30}\Big(\frac{1}{(I-\chi-\chi_\lambda)^2} - \frac{1}{(I-\chi)^2}\Big). \quad (12)$$

Here, I is the ionization potential, χ is the excitation potential of the lower level for the heavy metal atom. And χ_λ is the energy of a photon in the line, that is $\chi_\lambda = 1.24\times10^4/\lambda$, where λ is in Å.

4. ANALYSIS AND RESULTS

4.1. *Balmer lines*

The Balmer lines of the hydrogen-rich white dwarfs were analyzed using a χ^2 minimization technique and our cool hydrogen model atmospheres. The quoted uncertainties are only statistical (1σ) and do not take into account possible systematic effects in model calculations or data acquisition and reduction procedures.

4.2. *Sloan Colors*

Using the computed spectral grid, we have computed SDSS synthetic colors. For the white dwarf candidates for which we obtained spectra and for which SDSS photometry is available, we have compared the observed colors to the theoretical colors as a check of the temperatures obtained from the Balmer line profile fits. We have also calculated SDSS colors for a black-body spectrum for temperatures ranging from 4000 to 36000 K (in 1000 K intervals), and used these colors to obtain temperature estimates of DC white dwarfs.

The observed colors for a number of white dwarfs are compared to the synthetic $u-g$ versus $g-r$ colors in Figure 3 and $r-i$ versus $g-r$ colors in Figure 4. The $u-g/g-r$ diagram shows that the observed $u-g$ is larger than the $u-g$ calculated from the model atmospheres for

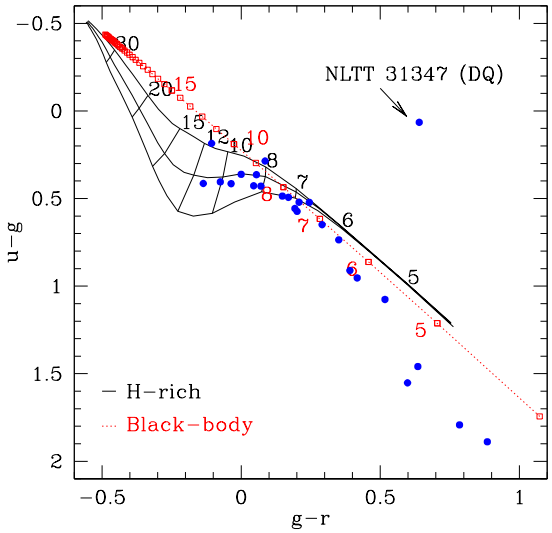

FIG. 3.— SDSS $u-g$ versus $g-r$ photometry of NLTT white dwarfs compared to synthetic colors of H-rich white dwarfs (*full line*) and blackbody (*dotted line*) colors. The DQ white dwarf NLTT 31347 is marked. The effective temperature is indicated in units of 1000 K and for H-rich colors $\log g = 7.0$, 8.0 and 9.0 from bottom to top.

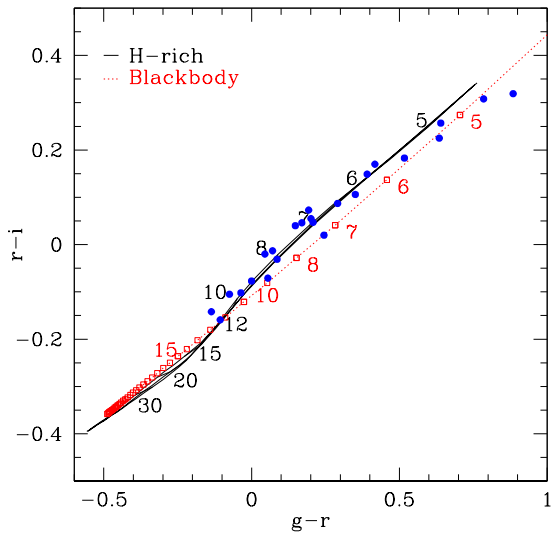

FIG. 4.— SDSS $r-i$ versus $g-r$ photometry of NLTT white dwarfs compared to synthetic colors of H-rich white dwarfs (*full line*) and blackbody (*dotted line*) colors. The effective temperature is indicated in units of 1000 K.

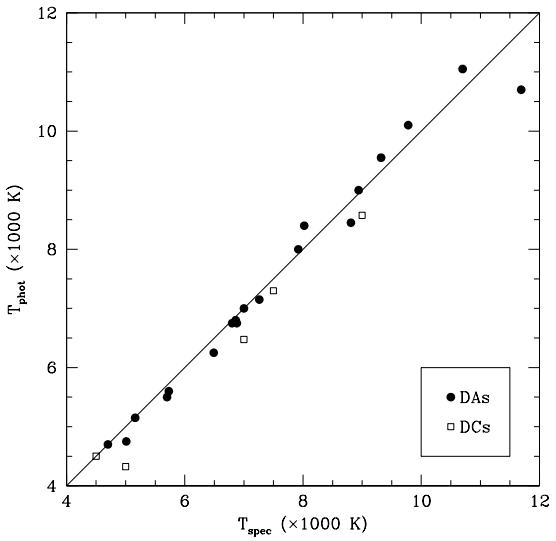

FIG. 5.— A comparison of the effective temperatures obtained using the spectra of stars (DA, *full circles*; DC, *open squares*) to the temperatures obtained using the $u-g/g-r$ and $r-i/g-r$ colors.

H-rich white dwarfs with temperatures less than $T_{\rm eff}$ = 7000 K (also noted by Kilic et al. 2006), hence implying some missing opacity in the u band. Bergeron (2001) suggests that a similar effect in the B band may be due to the bound-free opacity associated with the dissolved atomic levels of hydrogen, i.e., that following a bound-bound transition there is a probability that the upper level may be sufficiently perturbed by the surrounding particles that the electron will no longer be bound to the nucleus.

For the stars with SDSS *ugriz* photometry, the temperatures we obtained from spectroscopic fits were compared to the temperatures obtained using the $u-g/g-r$ and $r-i/g-r$ colors (Fig. 5). For DA white dwarfs, the label "spectroscopic fits" refers to temperatures obtained by fitting the Balmer line profiles with model spectra, and for DC white dwarfs the same label refers to temperatures obtained by comparing a black-body to the observed spectrum. The only point that appears to be in disagreement (i.e., the photometric temperature is lower than the spectroscopic temperature), is the ultramassive white dwarf NLTT 43827, which has a spectroscopic temperature of 11690 K. At this temperature the effect of gravity on the $u-g/g-r$ colors is the strongest and since we assumed $\log g = 8$ in our photometric temperature estimates, it is likely to effect the final temperature estimate for white dwarfs with significantly different surface gravities in this region of the color diagram. In Figure 5 the temperatures determined from the photometry appear to be slightly higher than those determined from spectroscopy for $T_{\rm eff} > 8000$ K and vice versa for $T_{\rm eff} < 8000$ K. This may be due to measurement errors or possibly to systematic errors in either spectroscopic (i.e., via the fitting of Balmer lines with model spectra) or photometric calibration.

4.3. *Interesting White Dwarfs*

Table 3 summarizes the results of the analyses of the white dwarfs. The table also includes white dwarfs from Vennes & Kawka (2003) and Kawka et al. (2004). The temperatures and surface gravities of the DA white dwarfs from these papers were remeasured with the improved synthetic spectra. For the cool DA white dwarfs the gravities went down significantly, in particular the gravity ($\log g = 9.00$) of NLTT 49985 went down to $\log g = 8.31$ and the high gravity should be discarded. Also the surface gravity of NLTT 31748 went down from $\log g = 8.40$ to $\log g = 7.85$.

NLTT 529— was observed by Kawka et al. (2004) and they classified this object as a cool DA white dwarf. We have reobserved this star and fitted the Balmer line profiles (Hα - H9) to obtain an effective temperature of 7380 ± 60 K and $\log g = 8.38 \pm 0.08$.

NLTT 3022— is also known as G 240-93 and PHL 3101, and was observed as part of the SDSS as SDSS J005438.3-095219.8. Kleinman et al. (2004) obtained $T_{\rm eff} = 8900$ K and $\log g = 8.20$. We fitted the Balmer lines with model spectra to obtain $T_{\rm eff} = 8810 \pm 50$ and $\log g = 8.11 \pm 0.06$ (see Figure 6).

NLTT 3915— is also known as LP 294-61 and its spectrum in Figure 1 shows that this is a cool DAZ white dwarf. We first fitted the Balmer lines (Hα and Hβ) with model spectra to obtain an effective temperature of $T_{\rm eff} = 5270 \pm 250$ and a surface gravity of $\log g = 8.36 \pm 0.60$. We then calculated a series of spectra with a varying abundance of sodium, for $T_{\rm eff} = 5270$ K and $\log g = 8.36$. We compared these synthetic spectra to the observed spectrum to find that logNa/H $= -8.1$.

NLTT 8651— is also known as GD 32 and was listed as a white dwarf suspect by Giclas et al. (1965), however it was not listed in the LWDC. Figure 1 shows that this is a cool DA white dwarf. We fitted the Balmer lines with model spectra to obtain an effective temperature of $T_{\rm eff} = 7040 \pm 90$ K and surface gravity of $\log g = 8.36 \pm 0.16$.

NLTT 10398— is also known as GD 44 and was listed as a white dwarf suspect by Giclas et al. (1965). Figure 2 shows this object to be a DC white dwarf. To obtain a temperature estimate we compared the optical/infrared colors ($V-J/J-H$) to blackbody colors and we only obtain a very uncertain termperature $T_{\rm eff} = 9900 \pm 4000$ K, but comparing the spectrum to a blackbody we obtain a temperature estimate of 11000 ± 1000 K.

NLTT 14307— is also known as G 84-26. Eggen (1968) obtained UBV photometry ($V = 15.12$, $B-V = +0.14$, $U-B = -0.62$) and classified it as a white dwarf based on these photometric colors. Figure 1 shows that this object is a DA white dwarf. We fitted the Balmer lines with model spectra and obtained an effective temperature of $T_{\rm eff} = 10850 \pm 80$ K and surface gravity of $\log g = 9.15 \pm 0.06$.

NLTT 17285— is also known as LP 661-15 and it was not listed in the LWDC. Figure 2 shows this object to be a DC white dwarf. We obtained a temperature estimate of $T_{\rm eff} = 5300 \pm 1100$ by comparing the optical/infrared colors ($V-J/J-H$) to calculated blackbody colors. A comparison of the spectrum with a blackbody spectrum suggested a temperature of 6000 ± 500 K.

TABLE 3
White Dwarf Parameters and Kinematics.

NLTT		WD	Spectral type	$T_{\rm eff}$ (K)	$\log g$ (cgs)	M ($M_\odot$)	M_V (mag)	d (pc)	U, V, W (km s^{-1})
287	APO	0004+122	DC	6300^{+1500}_{-1100}	(8.0)	(0.57)	13.91	26	-14, -33, -19
529	APO	0008+423[a]	DA	7380 ± 60	8.38 ± 0.08	0.83 ± 0.05	13.96	18	20, 3, -10
3022	SDSS	0052−101	DA	8810 ± 50	8.11 ± 0.06	0.66 ± 0.04	12.86	58	59, 36, 6
3915	APO	0108+277	DAZ	5270 ± 250	8.36 ± 0.60	0.81 ± 0.37	15.41	14	21, 5, -3,
6275	APO	0150+256	DA	7530 ± 70	8.18 ± 0.11	0.70 ± 0.07	13.56	28	-12, -8, 19
8435	MSO/SSO	0233−242[a,b]	DC	5400 ± 500	(8.0)	(0.58)	14.65	17	49, -24, -1
8581	MSO	0236+259[b]	DA	5500 ± 500	(8.0)	(0.58)	14.67	21	-7, -24, 8
8651	APO	0237+315	DA	7040 ± 90	8.36 ± 0.16	0.82 ± 0.10	14.12	26	22, 10, -10
9933	APO	0304+317	DA	13300 ± 300	7.87 ± 0.10	0.53 ± 0.05	11.30	81	-23, -60, 10
10398	APO	0313+393	DC	11000 ± 1000	(8.0)	(0.58)	12.02	56	-4, -33, -16
14307	APO	0457−004	DA	10800 ± 80	9.15 ± 0.06	1.24 ± 0.02	14.09	17	17, -17, 10
14352	APO	0458−064	DA	7900 ± 100	8.65 ± 0.13	1.01 ± 0.08	14.19	33	28, -28, 4
17285	APO	0658−075	DC	5900 ± 1000	(8.0)	(0.57)	14.20	32	-9, 28, -4
18555	APO	0749+426	DC	4300 ± 300	(8.0)	(0.57)	16.20	18	9, -31, 8
18642	APO	0753+417	DA	6880 ± 70	8.62 ± 0.16	0.99 ± 0.10	14.68	24	5, -30, 0
19019	SDSS	0806+294	DA	7000 ± 70	8.12 ± 0.11	0.66 ± 0.07	13.78	29	23, -8, 24
19138	APO	0810+489[a]	DC	7300 ± 100	(8.0)	(0.57)	13.31	23	8, -23, 11
20165	SDSS	0842+382	DA	8020 ± 50	8.16 ± 0.06	0.69 ± 0.04	13.31	35	20, -28, 17
21241	SDSS	0910+410	DA	6860 ± 100	8.00 ± 0.25	0.59 ± 0.14	13.72	51	-23, -4, -27
27901	SDSS	1132+574	DC	8600 ± 200	(8.0)	(0.58)	12.73	61	-32, -47, 7
28772	SDSS	1148+544	DA	9780 ± 70	8.14 ± 0.06	0.68 ± 0.04	12.51	68	-73, -40, -13
28920	APO	1151+795	DA	10810 ± 100	8.23 ± 0.07	0.74 ± 0.04	12.30	52	-45, -33, -12
29233	APO	1157+438	DA	7920 ± 50	8.19 ± 0.07	0.71 ± 0.04	13.40	33	-28, -21, -1
30738	APO	1223+188	DC	6000 ± 700[c]	(8.0)	(0.57)	14.12	26	-5, -7, 5
31347	APO	1235+422	DQ	~ 6250	(8.0)	(0.57)	~ 15.4[d]	27	-52, 19, -7
31748	SSO	1242−105[a,b]	DA	8280 ± 80	7.85 ± 0.13	0.51 ± 0.06	12.72	22	-19, -20, 2
32390	SDSS	1254+613	DA	9320 ± 70	8.18 ± 0.08	0.71 ± 0.05	12.75	92	-44, -76, 35
32695	SDSS	1300−005	DA	10700 ± 80	8.22 ± 0.05	0.74 ± 0.03	12.32	80	-51, -33, 11
34264	SDSS	1327−013	DA	7260 ± 110	8.12 ± 0.19	0.67 ± 0.11	13.62	37	31, -23, -13
34564	APO	1333−054	DA	7790 ± 100	8.54 ± 0.19	0.94 ± 0.12	14.04	30	-19, -11, 16
35880	APO	1356+607	DC	6500 ± 100	(8.0)	(0.57)	13.77	59	-63, -39, 20
38499	APO	1447−190	DA	7660 ± 80	7.81 ± 0.15	0.49 ± 0.06	12.97	37	-21, -15, 37
40489	APO	1529+141	DA	5250 ± 200	8.00 ± 0.50	0.58 ± 0.24	14.89	22	23, -7, 1
40607	MDM/SSO	1532+129[a]	DZ	~ 7500	(8.0)	(0.57)	13.20	24	14, -22, 12
40881	APO	1538+333	DA	8940 ± 100	8.44 ± 0.10	0.88 ± 0.06	13.35	22	-5, -2, 18
40992	APO	1540+236	DA	5730 ± 100	8.20 ± 0.35	0.71 ± 0.21	14.77	27	52, -25, -5
41800	SDSS	1559+534	DA	6800 ± 90	8.20 ± 0.20	0.72 ± 0.13	14.04	31	-36, 3, 14
42050	APO	1605+345	DA	5150 ± 350	~ 7.0	(0.18)	13.73	44	57, -18, 0
42153	APO	1607−250	DA	10420 ± 120	8.22 ± 0.09	0.74 ± 0.06	12.41	41	-2, 6, 43
43806	APO	1653+385	DAZ	5700 ± 240	8.28 ± 0.50	0.76 ± 0.30	14.91	15	31, -4, 4
43827	APO	1653+256	DA	11690 ± 140	9.35 ± 0.05	1.31 ± 0.01	14.29	33	37, -7, -7
43985	APO	1657+321	DA	6490 ± 80	8.76 ± 0.21	1.07 ± 0.13	15.20	22	28, -22, 23
44000	APO	1658+445	DA	5420 ± 100	7.68 ± 0.30	0.42 ± 0.12	14.30	31	38, -32, 39
44149	APO	1703+362	DC	4500 ± 400	(8.0)	(0.57)	15.83	27	34, 9, -14
44447	APO	1713+393	DAP	7000 ± 1000	magnetic	(0.59)	13.60	32	-18, 14, 13
44986	APO	1729+371	DAZ	9760 ± 70	9.19 ± 0.08	1.26 ± 0.03	14.54	22	31, -2, 0
45344	APO	1741+436	DA	5340 ± 160	7.84 ± 0.50	0.49 ± 0.20	14.59	34	43, -6, 6
45723	APO	1755+408	DC	5400 ± 600	(8.0)	(0.57)	14.65	33	-39, 21, 16
49985	SSO	2048−250[a]	DA	7630 ± 150	8.31 ± 0.31	0.79 ± 0.20	13.72	22	-1, -11, -14
50029	APO	2049−222	DC	9300 ± 1000	(8.0)	(0.58)	12.49	28	5, 22, 11
51103	APO	2119−017	DA	6440 ± 120	8.08 ± 0.27	0.64 ± 0.16	14.09	32	43, -24, 5
52404	SSO	2152−280[a]	DC	6500 ± 500	(8.0)	(0.57)	13.77	32	-15,27,-5
53177	MSO	2209−147[b,e]	DA	7920 ± 100	7.84 ± 0.30	0.50 ± 0.12	12.89	28	-21, 12, -7
53447	APO	2215+368	DC	4750 ± 250	(8.0)	(0.57)	15.44	20	-30, -1, -10
53468	SSO	2215−204[a]	DA	15120 ± 500	7.75 ± 0.15	0.48 ± 0.05	10.89	76	-69,15,-35
53996	APO	2227+232	DA	5000 ± 500	~ 7.0	(0.18)	13.92	64	-9, -40, -77
54047	APO	2228+151	DA	5580 ± 260	8.68 ± 0.58	1.02 ± 0.37	15.70	27	-57, 5, -9
55932	SSO	2306−220[a]	DA	14810 ± 260	7.86 ± 0.08	0.53 ± 0.04	11.08	33	-28, -25, -14
56122	APO	2309+129	DA	5010 ± 200	7.48 ± 0.60	0.33 ± 0.18	14.45	37	53, -15, -14
56805	MSO	2322+137[b]	DA	4700 ± 300	~ 7.0	(0.18)	14.27	20	-23 0, 4
58283	APO	2350+205	DA	7380 ± 50	7.95 ± 0.10	0.56 ± 0.06	13.31	45	6, -27, -28

[a]Also in Kawka et al. (2004).
[b]Also in Vennes & Kawka (2003).
[c]Possible binary, T_{eff} estimate from $V - J/J - H$ diagram.
[d]See text.
[e]Double degenerate system.

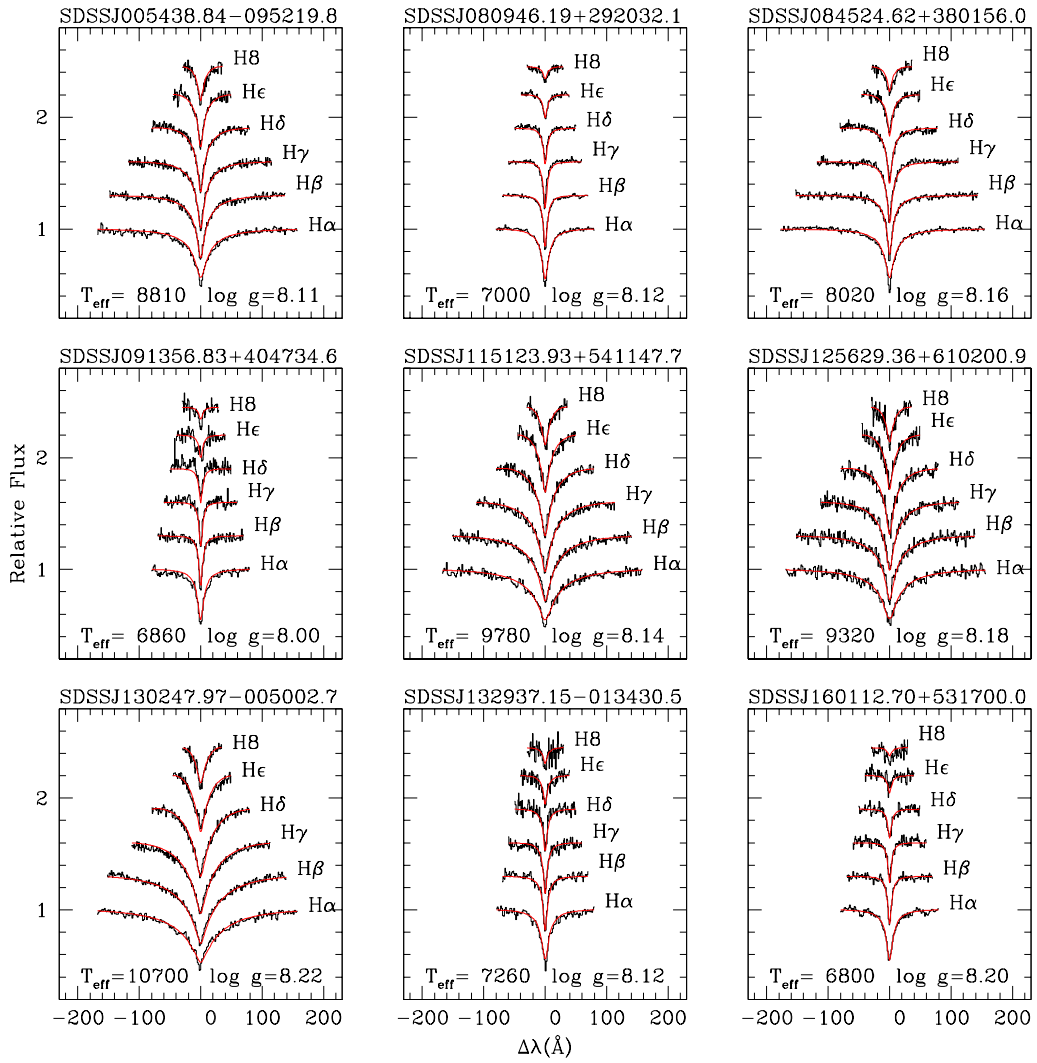

FIG. 6.— Balmer line profiles of NLTT white dwarfs with SDSS spectra compared to synthetic spectra.

NLTT 18555— is also known as LP 207-50. Figure 2 shows this object to be a DC white dwarf. SDSS photometry is available for this star (SDSS J075313.27+423001.5) and comparing the $u-g/g-r$ and $r-i/g-r$ to blackbody colors provides an estimate of the temperature of $T_{\rm eff} = 4300 \pm 300$ K. A comparison of the spectrum to a blackbody spectrum suggests a temperature of $T_{\rm eff} = 5000 \pm 1000$ K. Given that the infrared photometry has large uncertainty in the H band, we will adopt the temperature obtained using SDSS colors.

NLTT 18642— is also known as LP 207-55 and was also included in the Kiso Survey for ultraviolet objects (KUV07531+4148). Wegner & Swanson (1990) classified this object as NHB (i.e., stars with a HI dominated spectrum that could either be normal main-sequence or a horizontal-branch star). Figure 1 shows that this object is a cool DA white dwarf. We fitted the Balmer lines with model spectra to obtain an effective temperature of $T_{\rm eff} = 6880 \pm 70$ K and surface gravity of $\log g = 8.62 \pm 0.16$. The available SDSS colors ($u-g/g-r$ and $r-i/g-r$) implies a temperature of 6750 ± 200 K and confirms the temperature obtained from the spectral fit.

NLTT 19019— is also known as LP 311-2 and GD 262, and was observed as part of the SDSS as SDSS J080946.19+292032.1. It was listed as a white dwarf suspect Giclas et al. (1965). We fitted the Balmer lines with model spectra to obtain $T_{\rm eff} = 7000 \pm 70$ and $\log g = 8.12 \pm 0.11$ (see Figure 6).

NLTT 19138— was observed by Kawka et al. (2004) who classified this object as a DC white dwarf. We have reobserved this star and confirm this classification. The broad absorption features observed by Kawka et al. (2004) were not detected in the present observations. A comparison of the spectrum to a blackbody resulted in a temperature estimate of 7500 K. Using the available SDSS photometry for this object, we compared the observed colors ($u-g/g-r$ and $r-i/g-r$) to calculated colors for a black-body to obtained a temperature estimate of $T_{\rm eff} = 7300 \pm 100$ K, which is the temperature we adopt.

NLTT 20165— was observed as part of the SDSS as SDSS J084524.6+380156.0. It was also observed spectroscopically as follow up of the KISO survey as KUV 08422+3813 by Wegner & McMahan (1988), who observed a hydrogen dominated spectrum and suggested that it may be normal main-sequence or horizontal branch star. This star was not listed in the LWDC. The SDSS spectrum shows this to be a DA white dwarf. We fitted the Balmer lines with model spectra to obtain an effective temperature of $T_{\rm eff} = 8020 \pm 50$ K and a surface gravity of $\log g = 8.16 \pm 0.06$ (see Figure 6).

NLTT 21241— is also known as LP 210-58 and was observed as part of the SDSS as SDSS J091356.83+404734.6. The SDSS spectrum shows this object is a DA white dwarf. We fitted Balmer line profiles with model spectra to obtain an effective temperature of $T_{\rm eff} = 6860 \pm 100$K and a surface gravity of $\log g = 8.00 \pm 0.25$ (see Figure 6).

NLTT 27901— is also known as GD 311, LP 94-285 and LB 2052 and was observed as part of the SDSS as SDSS J113534.61+572451.7. It was included in the list of white dwarf suspects by Giclas et al. (1967). The SDSS spectrum shows this star to be a DC white dwarf. Comparing this spectrum to a blackbody, we obtained a temperature estimate of 9000 K. Using χ^2 minimization we compared the SDSS colors ($u-g/g-r$ and $r-i/g-r$) to blackbody colors to obtain a temperature estimate of $T_{\rm eff} = 8600 \pm 200$ K.

NLTT 28772— is also known as LP 129-587, G197-35 and it was observed spectroscopically by Liebert & Strittmatter (1977) who classified it a DA white dwarf. Weidemann & Koester (1984) using multichannel photometry, obtained an estimate of the temperature and surface gravity, $T_{\rm eff} = 8970$ K and $\log g = 7.99$. This white dwarf is the common proper motion companion to LP 129-586 and was observed as part of the SDSS as SDSS J115123.93+541147.7. We fitted the Balmer lines of the SDSS spectrum with model spectra to obtain an effective temperature of $T_{\rm eff} = 9780 \pm 70$ K and a surface gravity of $\log g = 8.14 \pm 0.06$ (see Figure 6).

NLTT 29233— is also known as G122-61. Eggen (1968) obtained UBV photometry ($V = 15.71$, $B-V = +0.30$, $U-B = -0.57$) and classified it as a white dwarf star. A low-dispersion spectrum in the blue was obtained as part of the Case Low-Dispersion Northern Sky Survey as CBS 451 (Pesch et al. 1995). It was classified as a featureless spectrum, Figure 1 shows that NLTT 29233 is a cool DA white dwarf. We fitted Balmer line profiles with model spectra to obtain an effective temperature of $T_{\rm eff} = 7920 \pm 50$ K and surface gravity of $\log g = 8.19 \pm 0.07$.

NLTT 30738— is also known as LP 435-109 and was not listed in the Luyten White Dwarf Catalog. Our spectroscopic observations revealed this object to be a DC white dwarf. We also observed weak Hα emission, suggesting that this may be close binary system. Comparison of optical-infrared photometry ($J-H/V-J$) to blackbody colors we obtain an effective temperature of 6400 K. However, if a companion is present, then this temperature estimate is most likely to be inaccurate.

NLTT 31347— is the high-proper motion object LHS 5222 (LP 217-47) which in Figure 1 is shown to be a DQ white dwarf. NLTT 31347 was also observed as part of the SDSS as SDSS J123752.12+415625.8. NLTT 31347 appears very similar to the white dwarf GSC2U J131147.2+292348 (Carollo et al. 2002). Two temperature estimates are available for GSC2U J131147.2+292348, $T_{\rm eff} = 5120 \pm 200$ K (Carollo et al. 2003) and $T_{\rm eff} = 5200$ K (Dufour et al. 2005). We compared the SDSS colors ($u-g/g-r$) to the theoretical colors for DQ white dwarfs at $\log g = 8$ presented in Dufour et al. (2005) to obtain a temperature estimate of $T_{eff} = 6250$ K with $\log C/He = -5$. Therefore, NLTT 31347 is one of the coolest DQ white dwarfs.

NLTT 32695— is also known as LP 616-70 and was observed as SDSS J130247.9-005002.7 in the SDSS. The SDSS spectrum shows this object to a DA white dwarf. We fitted the Balmer line profiles with model spectra to obtain $T_{\rm eff} = 10700 \pm 80$ K and $\log g = 8.22 \pm 0.05$. Kleinman et al. (2004) obtained $T_{\rm eff} = 10655$ K and $\log g = 8.33$ (see Figure 6) and Mukadam et al. (2004)

observed this star for variability, they did not find this object to vary.

NLTT 35880— is also known as LP97-430. Figure 1 shows that this is DC white dwarf. This star was observed in the SDSS and *ugriz* photometry is available for this object. Comparing the photometric colors $(u-g/g-r)$ to blackbody colors, we obtain an effective temperature of $T_{\rm eff} = 6500 \pm 100$ K.

NLTT 38499— is also known as LP 801-14 and was observed as part of the Edinburgh-Cape Survey (EC 14473−1901) and was classified as a sdB (Kilkenny et al. 1997). Figure 1 shows this object to be cool DA white dwarf rather than a sdB. We fitted the Balmer line profiles with model spectra to obtain $T_{\rm eff} = 7660 \pm 80$ K and $\log g = 7.81 \pm 0.15$. UBV photometry from the EC survey places this object on the white dwarf sequence with a temperature of ~ 7500 K.

NLTT 40489— is also known as LP 503-7 and was listed as GD 184 in the list of suspected white dwarfs by Giclas et al. (1965). Figure 1 shows this to be a cool DA white dwarf, fitting Balmer line profiles with model spectra resulted in an effective temperature of 5250 ± 200 K and surface gravity of $\log g = 8.0 \pm 0.5$. Due to the white dwarf being very cool, only the lines of Hα and Hβ can be seen and hence fitted.

NLTT 40881— is also known as LP 273-64, LTT 14655 and GD 187 and is listed as a white dwarf suspect by Giclas et al. (1965) but was not listed in the LWDC. Figure 1 shows that this is a DA white dwarf. We fitted the Balmer line profiles with model spectra to obtain $T_{\rm eff} = 8940 \pm 100$ K and $\log g = 8.44 \pm 0.10$.

NLTT 40992— is also known as LP 384-38. Figure 1 shows that this is a cool DA white dwarf. Fitting the Balmer line profiles with synthetic spectra we obtain $T_{\rm eff} = 5730 \pm 100$ K and $\log g = 8.20 \pm 0.35$. Again, due the weak Balmer lines in cool white dwarfs, only Hα and Hβ were used in the spectral fit.

NLTT 41800— is also known as G 202-26 and was not included in the LWDC. It was observed as SDSS J160112.70+531700.0 in the SDSS. This object was included in the SDSS 1st Data Release of white dwarfs (Kleinman et al. 2004), however they quoted an estimate of the temperature (~ 6700 K) with a note that the fit was unsatisfactory. Using the SDSS spectrum, we fitted the Balmer line profiles with model spectra to obtain $T_{\rm eff} = 6800 \pm 90$ K and $\log g = 8.20 \pm 0.20$ (see Figure 6).

NLTT 42050— is also known as LP 274-53. Figure 1 shows that this is a cool DA white dwarf. Due to the limited signal to noise ratio, we only fitted the Hα and $H\beta$ line profiles to obtain an effective temperature of $T_{\rm eff} = 5160 \pm 150$ and a surface gravity of $\log g = 7.0 \pm 0.6$. To check these values we used the available SDSS photometry to obtain a temperature estimate of $T_{\rm eff} = 5150 \pm 350$ K. We then compared synthetic spectra at different gravities ($\log g = 7.0$, 8.0 and 9.0), a visual inspection shows that a low surface gravity is required to match the Hα profile. We also performed a Balmer line fit assuming $\log g = 8.0$ for which we obtained an effective temperature of 5400 K.

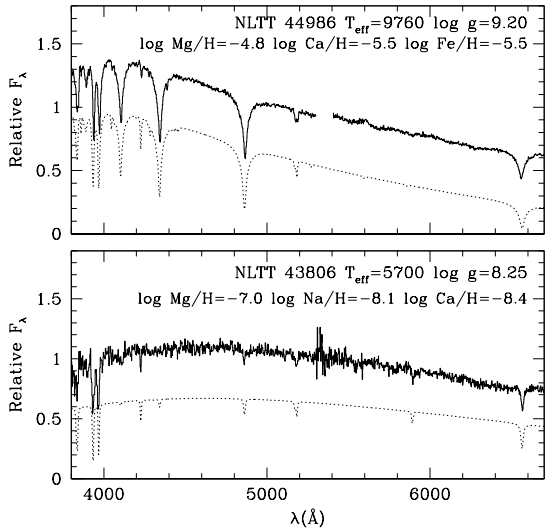

FIG. 7.— (*Top*) The observed spectrum of NLTT 44986 (*full line*) normalized at 4580 Å compared to a synthetic spectrum (*dotted line*) with abundances of $\log {\rm Mg/H} = -4.8$, $\log {\rm Ca/H} = -5.5$, and $\log {\rm Fe/H} = -5.5$. (*Bottom*) The observed spectrum of NLTT 43806 (*full line*) normalized at 5580 Å compared to a synthetic spectrum (*dotted line*) with abundances of $\log {\rm Mg/H} = -7.0$, $\log {\rm Na/H} = -8.1$ and $\log {\rm Ca/H} = -8.4$. The model spectra have been shifted downward by 0.4.

NLTT 42153— is also known as LP 861-31 and was recovered in the Yale/San Juan Southern Proper-Motion (SPM) program and is listed in the SPM Catalog 2.0 ($V = 15.24 \pm 0.11$, $B = 15.46 \pm 0.05$). Figure 1 shows this object to be a DA white dwarf. We fitted the Balmer line profiles with model spectra to obtain $T_{\rm eff} = 10420 \pm 120$ K and $\log g = 8.22 \pm 0.09$.

NLTT 43806— is also known as LP 276-33. Figure 1 shows this object to be a cool DAZ white dwarf. Table 4 presents the line identification of the most prominent heavy element lines. We first fitted the Balmer line profiles (Hα and Hβ) with pure hydrogen model spectra to obtain $T = 5700 \pm 240$ K and $\log g = 8.28 \pm 0.5$. We then calculated a series of spectra with varying abundance of sodium, calcium and magnesium, for $T = 5700$ K and $\log g = 8.25$. We compared these synthetic spectra to the observed spectrum to find that $\log {\rm Na/H} = -8.1$, $\log {\rm Ca/H} = -8.4$, and $\log {\rm Mg/H} = -7.0$. The large uncertainty in the surface gravity does not have significant effect on the abundance measurements. The uncertainty in the abundance measurements is 0.1 dex for all three heavy elements. The new results supersede our previous results published in Kawka & Vennes (2005). Figure 7 shows the observed spectrum compared to a synthetic spectrum with the computed abundances. At 5700K, NLTT 43806 is possibly one of the coolest DAZ ever observed. The abundance ratio Mg/Ca = 32 is comparable to other measurements (Zuckerman et al. 2003), but the the measured calcium abundance in NLTT 43806 is above the trend portrayed by Zuckerman et al. (2003).

NLTT 43827— is also known as LP 387-21. Figure 1 shows this object to be a DA white dwarf. We fitted the Balmer line profiles with model spectra to obtain $T_{\rm eff} = 11690 \pm 140$ K and $\log g = 9.35 \pm 0.05$. The

TABLE 4
Line Identifications of NLTT 43806.

λ (Å)	Element
3835.30[a]	MgI
3933.66	CaII
3968.47	CaII
4226.73	CaI
5178.14[b]	MgI
5892.94[c]	NaI

[a]Blend of 3832.30 Å and 3838.29 Å lines.
[b]Blend of 5172.68 Å and 5183.60 Å lines.
[c]Blend of 5889.95 Å and 5895.92 Å lines.

TABLE 5
Line Identifications of NLTT 44986.

λ (Å)	Element
3835.30[a]	MgI
3933.66	CaII
3968.47	CaII
4045.81	FeI
4226.73	CaI
4271.76	FeI
4383.54	FeI
5178.14[b]	MgI

[a]Blend of 3832.30 Å and 3838.29 Å lines.
[b]Blend of 5172.68 Å and 5183.60 Å lines.

temperature and surface gravity of NLTT 43827 places it outside the ZZ Ceti instability strip (Gianninas et al. 2005). However, due to its very high mass it remains interesting in defining the strip at high-gravity.

NLTT 43985— is also known as LP 331-27. Figure 1 shows that this is a cool DA white dwarf. Fitting the Balmer line profiles with synthetic spectra we obtain $T_{eff} = 6490 \pm 100$ K and $\log g = 8.76 \pm 0.20$. SDSS photometry ($u-g/g-r$ and $r-i/g-r$) results in a temperature of 6250 ± 200 K which is in agreement with the spectroscopic determination.

NLTT 44000— is also known as G 203-39 and it is not included in the LWDC. Figure 1 shows this to be a cool DA white dwarf. Fitting Balmer line profiles (Hα to Hγ) to model spectra we obtained $T_{\rm eff} = 5420 \pm 100$ K and $\log g = 7.68 \pm 0.30$.

NLTT 44149— is also known as LP 276-48. Figure 2 shows that this is a DC white dwarf. Fitting SDSS colors ($u-g/g-r$ and $r-i/g-r$) to blackbody colors results in an estimate of the temperature of $T_{\rm eff} = 4500 \pm 400$ K. A blackbody fit to the spectrum also results in a temperature of 4500 K. At this temperature the Balmer lines are very weak and a higher signal-to-noise ratio is required to conclude whether this is hydrogen- or helium-rich white dwarf. A comparison of the SDSS colors to synthetic H-rich colors also results in a temperature of 4500 K, however the lower limit of our synthetic colors grid is 4500 K.

NLTT 44447— is also known as LP 226-48. Figure 1 shows this object to be a cool magnetic DA white dwarf. Due to the Zeeman split Balmer lines, profile fitting would result in an inaccurate temperature and gravity. Therefore assuming $\log g = 8.0$ we compared $V-J/J-H$ to hydrogen-rich synthetic colors to obtain a temperature estimate of 7000 K. The Zeeman splitting corresponds to a magnetic field of 1.3 MG.

NLTT 44986— is also known as EG 545 or GD 362 and is listed as a white dwarf suspect by Giclas et al. (1967), however it was not included in the LWDC. Greenstein (1980) observed this star and classified it as a DA with a possible dK companion based on multichannel spectrophotometry. This object was also observed as part of the Palomar-Green survey (PG 1729+371: Green, Schmidt & Liebert 1986) and classified "sd". Figure 1 shows this object to be a cool DAZ white dwarf with no evidence for a companion. Table 5 presents the line identifications of the most prominent heavy element lines. We first fitted the Balmer line profiles with pure hydrogen model spectra to obtain $T_{\rm eff} = 9760 \pm 70$ K and $\log g = 9.19 \pm 0.08$. We then calculated spectra with varying abundances of calcium, magnesium and iron at $T = 9760$ K and $\log g = 9.20$. We compared these spectra to the observed spectrum to find that $\log {\rm Mg/H} = -4.8$, $\log {\rm Ca/H} = -5.5$, and $\log {\rm Fe/H} = -5.5$. Figure 7 shows the observed spectrum compared to a synthetic spectrum with the computed abundances. This star was also recently observed by Gianninas et al. (2004) and determined $T_{\rm eff} = 9740 \pm 50$ K and $\log g = 9.12 \pm 0.07$ with abundances $\log {\rm Mg/H} = -4.8$, $\log {\rm Ca/H} = -5.2$, and $\log {\rm Fe/H} = -4.5$. which is in agreement with our determinations except for the Fe abundance, for which we obtained a value a factor of 10 lower. Infrared observations of NLTT 44986 showed that it has significant excess from the K-band to the N-band and the presence of a debris disk around the ultra-massive white dwarf (Becklin et al. 2005; Kilic et al. 2005).

NLTT 45344— is also known LP 227-31. Figure 1 shows this object to be a cool DA white dwarf. Fitting Balmer lines (Hα to Hγ) to model spectra we obtained an effective temperature of $T_{\rm eff} = 5340 \pm 160$ and surface gravity of $\log g = 7.84 \pm 0.50$.

NLTT 45723— is also known LP 228-12. Figure 2 shows this object to be a DC white dwarf. Using the optical/infrared colors ($J-H/V-J$) we estimate a temperature of 5400 ± 600 K. Fitting a black-body to the spectrum we obtained a temperature of 5900 ± 100 K. Combining the two results we will adopt a temperature of 5890 ± 100 K.

NLTT 50029— is also known as LP 872-48. Beers et al. (1992) obtained a spectrum (BPS CS 22880-0126) as part of the spectroscopic follow-up of a selected sample of objects from the HK-survey. Based on UBV photometry ($V = 15.00$, $B-V = 0.17$, $U-B = -0.60$) they estimated a temperature of 12600 K. They classified the object as a DC white dwarf. Figure 2 confirms this clas-

sification. Using optical/infrared colors we estimate a temperature of 9600 K. Fitting a black body to the spectrum we estimate a temperature of 9500 K.

NLTT 53177— was observed by Vennes & Kawka (2003) and classified as a DA. We refitted the star to obtain $T_{\rm eff} = 7920 \pm 100$ K and $\log g = 7.82 \pm 0.30$. However, Karl et al. (2003) found NLTT 53177 (also HE 2209-1444) to be a short-period ($P_{\rm orb} = 0.276928 \pm 0.000006$ day) double degenerate system comprised of two white dwarfs with similar similar temperatures ($T_{\rm eff}$ = 8490, 7140 K) and equal mass ($M = 0.58 M_{\odot}$). The spectrum reported in Vennes & Kawka (2003) was of low-resolution and hence would not reveal the line core splitting; high resolution spectroscopy (i.e., echelle) such as that carried out by Karl et al. (2003) is required. Therefore there may be more double degenerates in our sample. Also note that our temperature determination appears close to the average temperature of the two components (Karl et al. 2003).

NLTT 53447— is also known as LP 287-39. Figure 2 shows this to be a DC white dwarf, fitting a black-body to this spectrum we obtain a temperature estimate of 4500 ± 200 K. Using the $J - H/V - J$ diagram we obtain a temperature of 5000 K, therefore we will adopt a temperature of 4750 K.

NLTT 53996— is also known as LP 400-6. Figure 2 shows this to be a cool DA white dwarf. Due to the limited signal-to-noise ratio we obtained an effective temperature by comparing the $J - H/V - J$ colors to synthetic colors for H-rich white dwarfs to obtain $T_{\rm eff} = 5000 \pm 500$ K. We then compared synthetic spectra at different gravities ($\log g = 7.0$, 8.0 and 9.0), a visual inspection shows that a low surface gravity ($\log g \sim 7.0$) is required to match the Hα profile. We also repeated this procedure for $T_{\rm eff} = 4500$ and 5500 K and we conclude that the best fit temperature is 5000 K and therefore we will adopt $T_{\rm eff} = 5000 \pm 500$ K and $\log g = 7.0$.

NLTT 54047— is the high-proper motion star LHS 3821 (LP 520-28). Recently, Reid & Gizis (2005) obtained spectroscopy of this object and classified it a DC white dwarf. The spectrum shown in Figure 1 shows this to be a cool DA white dwarf. Fitting the Balmer lines to model spectra we obtained $T_{\rm eff} = 5580 \pm 260$ K and $\log g = 8.68 \pm 0.58$.

NLTT 56122— is also known as LP 522-17. Figure 1 shows this to be a cool DA white dwarf. We fitted the Balmer lines to model spectra to obtain $T_{\rm eff} = 5010 \pm 200$ K and $\log g = 7.48 \pm 0.68$. Comparison of SDSS colors ($u - g/g - r$ and $r - i/g - r$) to synthetic H-rich colors results in a temperature of $T_{\rm eff} = 4750 \pm 250$ K.

Our sample of DA white dwarfs comprises nine stars with $T_{\rm eff} \leq 5500$ K, and of those nine, six have surface gravities below $\log g = 8.0$. There is probably a selection effect in finding more low-gravity cool DA white dwarfs, because Hα is predicted to be weaker (i.e., shallower lines) at higher gravities, and we are likely to classify these stars as DC white dwarfs. Therefore, higher signal-to-noise spectroscopy is required for such objects. Also our analyses of cool objects may suffer from uncertainties because our models currently exclude the effect of molecular hydrogen (Hansen 1998; Saumon & Jacobson 1999).

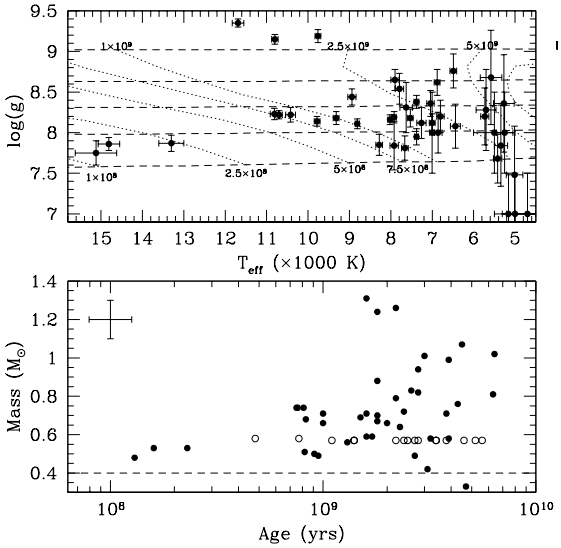

FIG. 8.— *Top:* Effective temperature and surface gravity distribution for the DA white dwarfs with the mass-radius relations ($0.4 - 1.2 M_{\odot}$ (in step of $0.2 M_{\odot}$)) of Benvenuto & Althaus (1999) for carbon interiors with a hydrogen envelope of $M_H/M_* = 10^{-4}$ and a metallicity of Z=0. *Bottom:* Masses and ages for the DA white dwarfs (*filled circles*). White dwarfs for which we have assumed $\log g = 8.0$ (i.e., DC, DQ, DZ) are shown as open circles. Typical errorbars for the masses and ages are shown at the top left corner of the figure.

5. DISCUSSION

The sample of rNLTT white dwarfs are old white dwarfs with ages of the order of 10^9 to 7×10^9 years. Figure 8 shows the effective temperature versus surface gravity of the DA white dwarfs compared to the mass-radius relations of Benvenuto & Althaus (1999), as well as the masses and ages for all the white dwarfs. No independent gravity measurements are available for non-DA white dwarfs and for the ultra-cool DA white dwarf NLTT 8581, and we simply assumed $\log g = 8$. Three objects (NLTT 14307, NLTT 43827, and NLTT 44986) have masses in excess of $1.2 M_{\odot}$ and belong to a sequence of high-mass white dwarfs also identified in EUV surveys (Vennes et al. 1997) and in common-proper motion surveys (Silvestri et al. 2001). Note also that three cool white dwarfs ($T_{eff} < 5200$K) also seem to be characterized by a low surface gravity ($\log g \sim 7$); the low surface gravity was diagnosed by their relatively strong Hα line strengths for their assigned effective temperatures. For the remaining 37 DA white dwarfs, the mass average and dispersion are $< M >= 0.69 M_{\odot}$ and $\sigma_M = 0.17 M_{\odot}$ which is slightly higher than the mass average ($< M >= 0.61 M_{\odot}$) of the H-rich subsample of Bergeron (2001). The distribution among various spectral types follows established trends. First, 45 objects (74%) from the present selection of 61 white dwarfs are hydrogen-rich, three are DAZ white dwarfs (NLTT 3915, NLTT 43806 and NLTT 44986). For at least three of the new DA white dwarfs the classification is primarily secured by the presence of Hα, which underlines the importance of obtaining red spectroscopy for a proper classification of cool white dwarfs. We suspect that a few

DC white dwarfs in the McCook & Sion (1999) catalog of spectroscopically identified white dwarfs may turn out to be DA white dwarfs. Some 14 objects are classified as DC white dwarfs (23%) and the two remaining objects consist of a new DQ white dwarf (NLTT 31347) and the DZ white dwarf NLTT 40607 (Kawka et al. 2004). For comparison, we determined the composition of 200 well-studied rNLTT white dwarfs using the McCook & Sion (1999) catalog: some 134 objects (67%) received a primary label "DA", 14 received the label "DB" (7%), 15 are DQ (8%), 11 are "DZ" (5%), and in last resort 26 received the label "DC" (13%). Combining the two data sets ($N = 261$), 69% of rNLTT white dwarfs are spectral type DA, and 31% non-DA. The DA:non-DA number ratio varies as a function of temperatures. By dividing the survey in the temperature bins < 6, $6 - 8$, $8 - 10$, and $10 - 12 \times 10^3$K, we observe a varying ratio 1.5:1, 3.6:1, 3.5:1, and 5:1, respectively. The ratio increases sharply with effective temperatures. The result of this proper motion survey are to be contrasted with the result of the parallax survey of Bergeron et al. (2001) who estimated DA:non-DA ratios varying from 1.2:1 in the < 6 bin, to 2:1 in a sparsely populated $8 - 10$ bin. The number of DC white dwarfs are markedly lower in the present proper motion survey. The DA:non-DA ratio in < 6 bin is only a lower limit, since for many white dwarfs in this bin it is very difficult to distinguish between H-or He-rich atmospheres without infrared photometry. For many of the objects accurate infrared photometry is required to ascertain the classification. Note that in this proper motion survey we selected the brighter candidates for spectroscopic observations, and therefore there may exist a slight bias against DC white dwarfs which tend to be fainter than DA white dwarfs.

Over 150 white dwarf candidates from our original selection (Kawka et al. 2004) remain to be spectroscopically confirmed. Eight white dwarfs (NLTT 529, NLTT 3915, NLTT 8435, NLTT 14307, NLTT 18555, NLTT 43806, NLTT 53447 and NLTT 56805) in the present compilation are found at distances closer than 20 pc from the Sun and therefore contribute to the local census. Other nearby white dwarfs are potentially among these remaining ~ 150 white dwarf candidates. We evaluate that $\sim 7\%$ of these are likely to lie within 20pc of the Sun. We assumed that all of these candidates are white dwarfs for which we calculated their absolute magnitude using VJH photometry, and then determined their distance.

Most white dwarfs in the neighborhood of the Sun belong to the thin disk population, but a significant number of thick disk white dwarfs are expected. We have calculated the velocity components U,V and W using Johnson & Soderblom (1987) and assuming $v_{\rm rad} = 0$. We have calculated absolute magnitudes using the temperatures and surface gravities as described in the previous sections and listed in Table 3. We obtained the distances using the apparent magnitudes and the absolute magnitudes listed in Table 1 and Table 2. Figure 9 compares measured U and V to the 2σ velocity ellipse of the thin disk population, the 2σ ellipse of the thick disk population and the 1σ ellipse of the halo population (Chiba & Beers 2000). The following velocities are all expressed in km s^{-1}. All three distributions, UVW, were fitted with Gaussian functions, where $\sigma_U = 34$, $\sigma_V = 22$, $\sigma_W = 19$ and $< U >= -2$, $< V >= -13$, $< W >= 1$. Our velocity dispersions are in good agreement with those of a thin disk population ($\sigma_U = 34$, $\sigma_V = 21$, $\sigma_W = 18$ Binney & Merrifield 1998), however our $< V >= -13$ is only slightly more negative then their quoted value of $< V >= -6$ for normal stars in the thin disk. Hence, the measured velocity distributions imply that the majority of the objects in this study belong to the thin disk population.

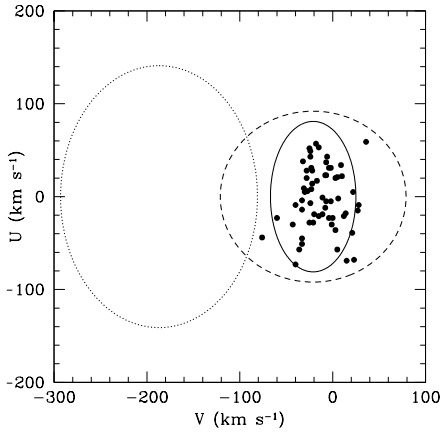

FIG. 9.— U vs. V diagram showing the white dwarfs listed in Table 3. The 2σ velocity ellipse of the thin disk population is shown (*full line*), along with the 2σ ellipse of the thick disk (*dashed line*), and the 1σ ellipse of the halo (*dotted line*) populations.

The local sample of white dwarfs should consist of a significant number of white dwarfs that belong to the thick disk population. Several estimates of the fraction of thick disk white dwarfs in the Solar neighborhood have been made, from $\sim 5\%$ (Hansen & Liebert 2003) up to 25% (Reid 2005). The main reason for the difference between the two values is that the first assumes a single power-law for the initial mass function, which produces more low-mass main-sequence stars and hence a small white dwarf mass-fraction in the disk (N_{WD}/N_{MS}). Reid (2005) used a two-component power law, which produces fewer low-mass main sequence stars and hence the white dwarf mass fraction for the thick disk will be higher. Therefore, the thick disk could contribute as much as 25% of the local white dwarfs.

It is difficult to disentangle thin versus thick disk populations solely based on the kinematics. A study of the distribution of white dwarfs in the UV plane led Kawka et al. (2004) to conclude that 5% of their sample of $N = 417$ white dwarf candidates extracted from the rNLTT catalog of Salim & Gould (2003) lay in a high-velocity tail and, therefore, may belong to the thick disk population. Kawka et al. (2004) used the V-velocity distribution which is most sensitive to the presence of thick disk white dwarfs which are characterized by a velocity dispersion twice the dispersion of thin disk white dwarfs ($\sigma_{\rm thick} = 50$ versus $\sigma_{\rm thin} = 21$). Therefore, the fraction of thick disk white dwarfs estimated by Kawka et al. (2004) is a lower limit, considering that several objects assimilated with the thin disk population may in fact be part of the bulk of the thick disk population only betrayed by its high-velocity tail. Similarly in this study of 61 objects, four objects in Figure 9 are clearly lying

outside the 2σ velocity ellipse of the thin-disk population. If these four objects were assumed to belong to the thick-disk, then the percentage of thick-disk white dwarfs in our sample would be 6.5% which is consistent with Hansen & Liebert (2003). Note that this is a lower limit.

6. SUMMARY

We have spectroscopically identified 49 new white dwarfs from the rNLTT survey of Salim & Gould (2003) in addition to the 12 white dwarfs from Vennes & Kawka (2003) and Kawka et al. (2004). Their proper motions range from 0.136 to $0.611''\mathrm{yr}^{-1}$ which is to be contrasted with the proper motions of suspected halo white dwarf candidates WD 0346+246 ($1.27''\mathrm{yr}^{-1}$) and PM J13420−3415 ($2.55''\mathrm{yr}^{-1}$). Some 45 objects from this sample are hydrogen rich white dwarfs for which we have determined effective temperatures and surface gravities fitting the Balmer lines to synthetic spectra. For 14 of the objects we provided a DC classification and estimated their temperature by comparing their spectra and photometric colors to a black body. Of the 45 hydrogen-rich white dwarfs, three display a high abundance of heavy elements (NLTT 3915, NLTT 43806 and NLTT 44986). One of these (NLTT 44986) is also an ultramassive white dwarf with a mass of $1.26M_{\odot}$, and another one is a magnetic white dwarf (NLTT 44447) with an estimate surface magnetic field of 1.3 MG. In our sample there is also one cool DQ white dwarf (NLTT 31347) with an estimated temperature of 5200 K and the cool DZ NLTT 40607 presented by Kawka et al. (2004).

Eight of the white dwarfs have distances that place them within 20 pc of the Sun, hence contributing toward the local census. Parallax measurements of the new nearby white dwarfs should be obtained in order to provide independent estimate of their radius and mass. We determined U,V and W space velocities for all 61 objects. The means and dispersions of U and V suggest that these objects belong to the thin disk. However, due to the overlap of the thick disk population distribution with the thin disk population distribution in the UV plane, some of the stars in our sample may belong to the thick disk. To help distinguish between thick and thin disk white dwarf populations, the z-component of the angular momentum J_z, the eccentricity of the orbit e and the Galactic orbit should be calculated (Pauli et al. 2005). Therefore, to obtain full information about the kinematics of the white dwarfs, accurate radial velocity measurements are necessary.

This research received financial support from the College of Science of the Florida Institute of Technology. A. Kawka is supported by GA ČR 205/05/P186. We thank Pierre Chayer for sharing APO observing time. Based on observations obtained with the Apache Point Observatory 3.5-meter telescope, which is owned and operated by the Astrophysical Research Consortium (ARC). We thank T. Oswalt, M. Wood, J. Kubat and and the referee for interesting comments.

Funding for the creation and distribution of the SDSS Archive has been provided by the Alfred P. Sloan Foundation, the Participating Institutions, NASA, the NSF, the U.S. Department of Energy, the Japanese Monbukagakusho, and the Max Planck Society. The SDSS Web site is http://www.sdss.org/. The SDSS is managed by the ARC for the Participating Institutions: The University of Chicago, Fermilab, the Institute for Advanced Study, the Japan Participation Group, The Johns Hopkins University, the Korean Scientist Group, Los Alamos National Laboratory, the Max-Planck-Institute for Astronomy, the Max-Planck-Institute for Astrophysics, New Mexico State University, University of Pittsburgh, Princeton University, the United States Naval Observatory, and the University of Washington.

REFERENCES

Becklin, E.E., Farihi, J., Jura, M., Song, I., Weinberger, A.J., & Zuckerman, B. 2005, ApJ, 632, L119
Beers, T.C., Preston, G.W., Shectman, S.A., Doinidis S.P., & Griffin, K.E. 1992, AJ, 103, 276
Bergeron, P. 2001, ApJ, 558, 369
Bergeron, P., Leggett, S. K., & Ruiz, M. T. 2001, ApJS, 133, 413
Bergeron, P., Wesemael, F., & Fontaine, G. 1991, ApJ, 367, 253
Bergeron, P., Wesemael, F., & Fontaine, G. 1992, ApJ, 387, 288
Benvenuto, O.G., & Althaus, L.G. 1999, MNRAS, 303, 30
Binney, J., & Merrifield, M. 1998, Galactic Astronomy (Princeton: Princeton Univ. Press)
Carollo, D., Bucciarelli, B., Hodgkin, S.T., Lattanzi, M.G., McLean, B.J., Morbidelli, R., Smart, R.L., Spagna, A., & Terranegra, L. 2005, A&A, submitted (astro-ph/0510638)
Carollo, D., Hodgkin, S.T., Spagna, A., Smart, R.L., Lattanzi, M.G.,McLean, B.J., & Pinfield, D.J. 2002, A&A, 393, L45
Carollo, D., Koester, D., Spagna, A., Lattanzi, M.G., & Hodgkin, S.T. 2003, A&A, 400, L13
Chiba, M., & Beers, T.C. 2000, AJ, 119, 2843
Cutri, R.M., et al. 2003, Explanatory Supplement to the 2MASS All Sky Data Release (Pasadena: Caltech)
Dufour, P., Bergeron, P., & Fontaine, G. 2005, ApJ, 627, 404
Eggen, O.J. 1968, ApJS, 16, 97
Fontaine, G., Villeneuve, B., & Wilson, J. 1981, ApJ, 243, 550
Gizis, J.E., & Reid, I.N. 1997, PASP, 109, 849
Green, R.F., Schmidt, M., & Liebert, J. 1986, ApJS, 61, 305
Greenstein, J.L. 1980, ApJ, 242, 738
Gianninas, A., Bergeron, P., & Fontaine, G. 2005, ApJ, 631, 1100
Gianninas, A., Dufour, P., & Bergeron, P. 2004, ApJ, 617, L57
Giclas, H.L., Burnham, R., & Thomas, N.G. 1965, Lowell Observatory Bulletin, 6, 155
Giclas, H.L., Burnham, R., & Thomas, N.G. 1967, Lowell Observatory Bulletin, 7, 49
Gray, D.F. 1992, The Observation and Analysis of Stellar Photospheres, 2nd Ed. (Cambridge: Cambridge Univ. Press)
Hambly, N.C., et al. 2001, MNRAS, 326, 1279
Hambly, N.C., Henry, T.J., Subasavage, J.P., Brown, M.A., & Jao, W.-C. 2004, AJ, 128, 437
Hambly, N.C., Smartt, S.J., & Hodgkin, S.T. 1997, ApJ, 489, L157
Hansen, B.M.S. 1998, ApJ, 520, 680
Hansen, B.M.S., & Liebert, J. 2003, ARA&A, 41, 465
Hintzen, P. 1986, AJ, 92, 431
Holberg, J.B., Oswalt, T.D., & Sion, E.M. 2002, ApJ, 571, 512
Hubeny, I., Hummer, D.G., & Lanz, T. 1994, A&A, 282, 151
Hummer, D.G., & Mihalas, D. 1988, ApJ, 331, 794
Johnson, D.R.H., & Soderblom, D.R. 1987, AJ, 93, 864
Karl, C.A., Napiwotzki, R., Nelemans, G., Christlieb, N., Koester, D., Heber, U., & Reimers, D. 2003, A&A, 410, 663
Kawka, A., Vennes, S., & Thorstensen, J.R. 2004, AJ, 127, 1711
Kawka, A., & Vennes, S. 2005, in 14th European Workshop on White Dwarfs, ASP Conf. Ser. Vol. 334, eds. D. Koester, & S. Moehler, 101
Kawka, A., Vennes, S., Wickramasinghe, D.T., Schmidt, G.D., & Koch, R. 2003, in White Dwarfs, NATO Science Series II: Mathematics, Physics and Chemistry (Kluwer), vol. 105, eds. de Martino, D., Silvotti, R., Solheim, J.-E., & Kalytis, R., 179

Kilic, M., Munn, J.A., Harris, H.C., Liebert, J., von Hippel, T., Williams, K.A., Metcalfe, T.S., Winget, D.E., & Levine, S.E. 2006, AJ, 131, 582
Kilic, M., von Hippel, T., Leggett, S.K., & Winget, D.E. 2005, ApJ, 632, L115
Kilkenny, D., O'Donoghue, D., Koen, C., Stobie, R.S., & Chen, A. 1997, MNRAS, 867
Kleinman, S.J., et al. 2004, ApJ, 607, 426
Lemke, M. 1997, A&AS, 122, 285
Lepine, S., & Shara, M.M. 2005, AJ, 129, 1483
Lepine, S., Shara, M.M., & Rich, R.M. 2002, AJ, 124, 1190
Lepine, S., Shara, M.M., & Rich, R.M. 2003, AJ, 126, 921
Lepine, S., Rich, R.M., & Shara, M.M. 2005, ApJ, 633, L121
Liebert, J. & Strittmatter, P.A. 1977, ApJ, 217, L59
Luyten, W.J. 1970, White Dwarfs (Minneapolis: Univ. Minnesota Press)
Luyten, W.J. 1977, White Dwarfs II (Minneapolis: Univ. Minnesota Press)
McCook, G. P., & Sion, E. M. 1999, ApJS, 121, 1
Mihalas, D. 1978, Stellar Atmospheres, 2nd Ed. (San Francisco: Freeman)
Mukadam, A.S., et al. 2004, ApJ, 607, 982
Pauli, E.-M., Napiwotzki, R., Heber, U., Altmann, M., & Odenkirchen, M. 2005, A&A, in press (astro-ph/0510494)
Pesch, P., Stephenson, C.B., & MacConnell, D.J. 1995, ApJS, 98, 41
Pravdo, S.H., et al. 1999, AJ, 117, 1616
Reid, I.N., et al. 2003, AJ, 126, 3007
Reid, I.N. 2005, ARA&A, 43, 247
Reid, I.N., & Gizis, J.E. 2005, PASP, 117, 676
Saumon, D., & Jacobson, S.B. 1999, ApJ, 511, L107
Salim, S., & Gould, A. 2002, ApJ, 575, L83
Salim, S. & Gould, A. 2003, ApJ, 582, 1011
Schöning, T. 1994, A&A, 282, 994
Schröder, K.-P., Pauli, E.-M., & Napiwotzki, R. 2004, MNRAS, 354, 727
Silvestri, N. M., Oswalt, T. D., Wood, M. A., Smith, J. A., Reid, I. N., & Sion, E. M. 2001, AJ, 121, 503
Subasavage, J.P., Henry, T.J., Hambly, N.C., Brown, M.A., Jao, W.-C., & Finch, C.T. 2005, ApJ, 130, 1658
Teegarden, B.J., et al. 2003, ApJ, 589, L51
Vennes, S., Thejll, P., Genova-Galvan, R., & Dupuis, J. 1997, ApJ, 480, 714
Vennes, S., & Kawka, A. 2003, ApJ, 586, L95
Wegner, G., & McMahan, R.K. 1988, AJ, 96, 1933
Wegner, G., & Swanson, S.R. 1990, AJ, 99, 330
Weidemann, V., & Koester, D. 1984, A&A, 132, 195,
Yong, D., & Lambert, D.L. 2003, PASP, 115, 22
Zuckerman, B., Koester, D., Reid, I. N., Hünsch, M. 2003, ApJ, 596, 477